A study of irradiation induced voids in dispersion hardened stainless Steel

Singh, Bachu Narain

Publication date:
1974

Document Version
Publisher's PDF, also known as Version of record

Risø Report No. 287

Risø Report No. 287

Danish Atomic Energy Commission

Research Establishment Risø

A Study of Irradiation Induced Voids in Dispersion Hardened Stainless Steel

by B. N. Singh

March 1973

Sales distributors: Jul. Gjellerup, 87, Sølvgade, DK-1307 Copenhagen K, Denmark

Available on exchange from: Library, Danish Atomic Energy Commission, Risø, DK-4000 Roskilde, Denmark

UDC 669.14.018.8:621.767:539.12.04

March 1973 Risø Report No. 287

A Study of Irradiation Induced Voids in Dispersion Hardened Stainless Steel

by

B. N. Singh

Danish Atomic Energy Commission
Research Establishment Risø
Metallurgy Department

Abstract

An "experimental" stainless steel with ultra-fine grains and with and without dispersions of fine oxide particles has been irradiated with 1 MeV electrons in a High Voltage Electron microscope; samples with and without implanted helium have been irradiated. It is shown that the nucleation of voids and the resultant volume swelling are severely reduced by decreasing the size of the grain under irradiation. A further reduction in swelling is obtained in the specimens containing dispersions of oxide particles. The implanted helium atoms increase the void number density in large grains but have very little effect in the small ones.

The present results are found to be consistent with a model based on the migration of point defects to grain boundaries giving rise to a grain size dependent vacancy concentration in the grain interior within a certain grain size range.

It is concluded that the grain refinement and dispersion of small particles lead to a highly swelling resistant material which may be considered as an attractive candidate material for the fast breeder reactor application.

ISBN 87 550 01 92 0

CONTENTS

1. INTRODUCTION

Since the first observation of irradiation induced voids in a reactor cladding by Cawthorne and Fulton[1], voids have been observed in a large variety of metals and alloys irradiated with neutrons, charged particles, and high energy electrons[2, 3]. When the energetic particles collide with target atoms during irradiation, sufficient energy is imparted to the target atoms to displace them permanently from their original lattice sites, creating vacancies and self-interstitials. At a given irradiation temperature, where both types of defects produced are mobile, the accumulation of vacancies necessary for the nucleation of voids depends primarily on the number, distribution, and type of defect-sinks present in the material.

It is generally believed that because of the presence of a large number of edge dislocations which act as biased sinks for self-interstitials[4-6], an excess of vacancy population is created during an irradiation experiment. As the irradiation continues the accumulation of vacancies produces a concentration level at which the nucleation of vacancy clusters becomes possible. The kinetics of the formation of such vacancy clusters which serve as void embryos has been treated theoretically by several authors[7-10]. Bullough and Perrin[11] have suggested that these vacancy clusters are stabilized by impurity gas atoms into a three-dimensional configuration of void nuclei against their collapse into a two-dimensional configuration of vacancy loops. These voids then grow during subsequent irradiation and produce volume swelling. This kind of irradiation induced dimensional instability in the reactor material is highly undesirable from the reactor design point of view.

The nature and the degree of damage produced during irradiation is a complex function of irradiation (flux, energy, temperature) and material variables (dislocations, grain or subgrain boundaries, particles, stacking faults etc.). The influence of only very few of these parameters on the voidage characteristics of different metals and alloys has been studied theoretically and/or determined experimentally.

The effect of grain size on swelling has been considered by Harkness and Li[12], who predicted that the swelling would be reduced in fine-grained material. The grain size dependence of the irradiation induced swelling arises from the property of grain boundaries that they act as neutral and unsaturable sinks for both vacancies and interstitials. The evidence of this lies in the fact that in quenched as well as in irradiated metals and alloys the formation of loops and voids is completely suppressed in the

vicinity of grain boundaries[3,13,14]. Recently, the author has reported some experimental results showing a drastic reduction in swelling in the case of grains smaller than about one micron[15].

The purpose of the present report is to describe and discuss in detail the damage behaviour of our experimental material and to demonstrate the grain size dependence of the irradiation induced swelling. It is shown that the void nucleation behaviour of our stainless steel, both with and without implanted helium, is critically dependent on grain size; the effect of non-coherent second phase particles is also considered. The dependence of void number density, void size, and void volume on grain size is explained by a model proposed herein.

2. MATERIAL AND EXPERIMENTAL PROCEDURE

The materials used in the present investigation were manufactured from pre-alloyed austenitic stainless steel powder of composition quoted in table 1. The finished products were obtained either in the form of extruded bar or extruded and hot-rolled sheet. The specimens are classified according to their composition, fabrication and heat-treatment as shown in table 2.

Table 1

Composition of pre-alloyed powder

Element	Fe	Ni	Cr	C	Mo	Nb	W	Si
Concentration (Wt. %)	Bal.	20	20	0.02	ND*	ND*	ND*	0.22

All heat-treatments were done in a vacuum of 10^{-6} torr for two hours. Thin films were prepared from the annealed samples by electro-polishing in ethanol with 20 v% perchloric acid at -20°C (see ref. 16 for details).

The microstructure of our experimental stainless steels RMS-1a and RMS-2a, after annealing at 800°C for 2 hrs. in vacuum and before irradiation are shown in fig. 1. It should be noted that in both cases the grain size is very small (e.g. between 0.3 and 1.0 μm); in general the specimens containing the dispersion of aluminium oxide particles had smaller grains than those without dispersions. The microstructures of RMS-1c and RMS-2b were essentially the same as that of RMS-1a and RMS-2a, respectively.

* Not detectable

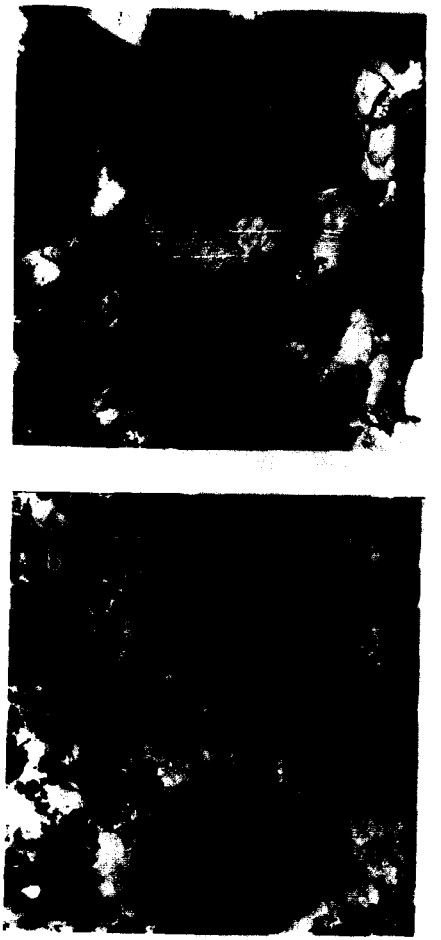

Fig. 1. 100 kv electron micrographs showing general structure: (a) RMS-1a, x 20,000 (b) RMS-2a, x 40,000.

Relatively large grains were obtained in RMS-1(b, d) by annealing them at 1150°C (see table 2).

In some selected thin films 10 ppm of helium was implanted at room temperature using 100 kV Heavy Ion Accelerator at A. E. R. E. Harwell (England). Thin films, both with and without helium, were irradiated at 1 MeV in the EM-7 Electron Microscope at Harwell; all irradiation experiments were carried out at 600°C. During irradiation a vacuum of $\sim 2\text{-}3 \times 10^{-7}$ torr was maintained around the specimen. The microscope current was adjusted to give a displacement rate of 5.16×10^{-3} dpa (displacement per atom) sec^{-1} within a 0.5 μm dia. circle on the specimen. For comparison purposes, a specimen of cast and solution treated (at 1050°C for 30 min.) AISI type 316 stainless steel* was irradiated under exactly the same conditions as our RMS-1 and RMS-2 stainless steels. The average grain size of the 316 stainless steel specimen was of the order of 50 μm.

Table 2

Specimen description

Designation	Description
RMS-1a	Composition as in table 1, extruded, annealed at 800°C
RMS-1b	Same as RMS-1a, but annealed at 1150°C
RMS-1c	Composition as in table 1, extruded and hot-rolled, annealed at 800°C
RMS-1d	Same as RMS-1c, but annealed at 1150°C
RMS-2a	Composition as in table 1, 1.0 w% Ti (powder), 5.0 v/o Al_2O_3 particles of 500 A° dia. (i.e. 0.76×10^{15} Al_2O_3 particles/cm^3) extruded and annealed at 800°C
RMS-2b	Same as RMS-2a, but no Ti, extruded and hot-rolled, annealed at 800°C

*The 316 stainless steel specimen was supplied by Mr. G. P. Walters, Harwell.

During irradiation the specimen structure was photographed at various stages. Swelling data were obtained by measuring the void size and counting the void number on micrographs with a total magnification of 86.5×10^3; Generally voids were counted and measured in the central region of the irradiated material in an area of 14 cm^2 on the micrographs (representing a circular region of the specimen of less than 0.5 μm in dia.). The thickness of the foil containing voids were measured from stereopairs of micrographs using a stereomicroscope. From these, the swelling ($\Delta V/V$) (where ΔV is the total volume of voids in the material of volume V), and the void concentration, C_v, can easily be obtained. In the computation of ($\Delta V/V$) the average void diameter, d_v, was always used.

3. RESULTS

3.1. Nucleation of Dislocation Loops and Voids

Agglomeration of point defects, created during an irradiation experiment, into defect clusters with black-dot contrast, produces the first microscopically observable damage in irradiated crystalline solids. Subsequently these black-dots grow into resolvable unfaulted or faulted dislocation loops. Since the displacement damage rate during electron irradiation used throughout the present investigation is very high (i.e. 5.16×10^{-3} dpa/sec), a rapid build-up of the damage is expected. Evidence of this fast damage rate is shown in fig. 2. In an undoped sample (i.e. without implanted helium), a large grain, with only a few grown-in dislocations, was selected after the specimen had been at 600°C in the microscope for about 2 hours. During the irradiation the specimen was photographed at intervals of one minute. Fig. 2 shows two of these exposures taken at $t_i = 0$, and $t_i = 1$ min. (t_i is the time of irradiation); the centre of the focused beam on the specimen was approximately at 0 (fig. 2a). Evidently, a sizeable number of defect clusters in the form of black-dots and unfaulted loops have already been formed at $t_i = 0$, i.e. during positioning and focusing of the grain. Fig. 2c shows a micrograph of a grain smaller than that in fig. 2a, in a doped sample containing 10 ppm. of helium, taken at $t_i = 0$ at 600°C; the centre of the beam in this case was focused in the centre of the grain. Again, evidence of defect clusters with black-dot contrast and resolvable dislocation loops is clear. In both cases some of the newly formed dislocation loops are associated with the grown-in dislocation lines. It should also be noted that in figs. 2(a-b) most of the loops

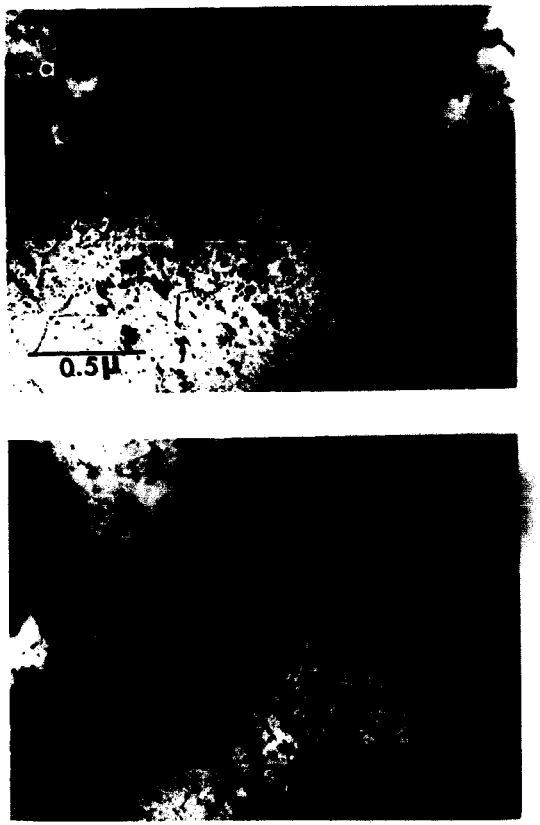

Fig. 2. 1 MeV electron micrographs of RMS-1 stainless steel at 600°C: (a) φt = 0, no helium, (b) 0.31 dpa (t_i = 1 min.), no helium, and (c) φt = 0, 10 ppm helium.

are aligned in a particular direction whereas in fig. 2c no such alignment of the loops exists.

Fig. 2c.

Although most of the loops in figs. 2 (a-b) are elongated, there are some loops which are nearly circular in shape and which in general are not associated with dislocations or grain boundaries. The elongated loops associated with dislocations or grain boundaries grew much faster than those which were isolated; the growth occurred predominantly in the direction of elongation. The growth in the width direction for both isolated loops and loops associated with dislocations and grain boundaries was, to a first approximation, very similar (fig. 3).

During irradiation of undoped and small grains of RMS-1 steel, in several cases voids were not observed up to a dose level of about 40 dpa; such an example is shown in fig. 4. The smallest size of the grain in which voids have been observed is 0.45 μm (see table 3). The void formation behaviour of undoped and relatively large grains is typified by fig. 5; the grain size in fig. 5 is 2.60 μm. Fig. 5c shows the voids formed in the type 316 (undoped) stainless steel at a dose level of 4.65 dpa; the grain size in this case is about 50 μm.

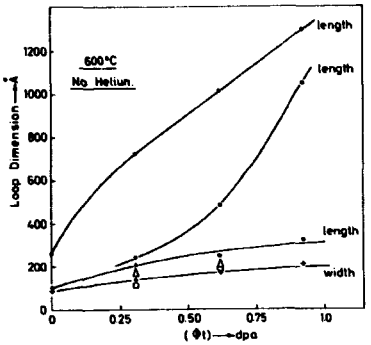

Fig. 3. Dislocation loop growth: Curve (1) - loops associated with grown-in dislocations, curve (2) - loops associated with grain boundaries, curve (3) - isolated loops, curve (4) - isolated loops (+) and loops associated with grain boundaries (□) and dislocations (Δ).

Fig. 4. 1 MeV electron micrographs of RMS-1a stainless steel (without helium) at 600°C; 18.91 dpa, $d_g \simeq 0.5$ μm.

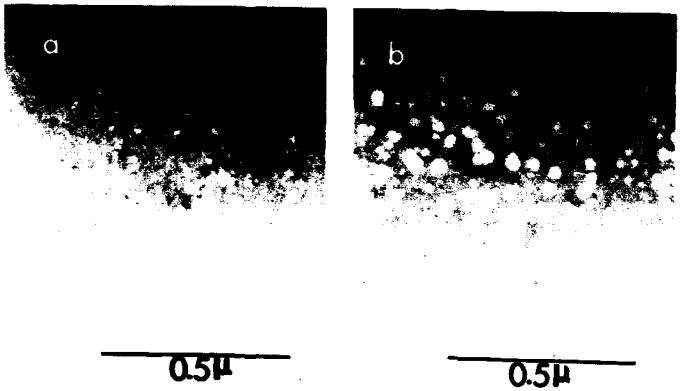

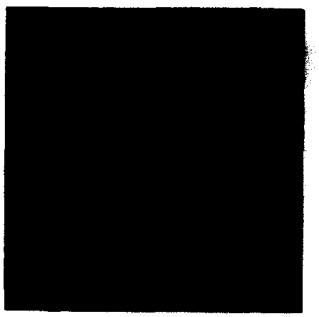

Fig. 5. Voids in RMS-1b (d_g = 2.60 μm) and type 316 stainless steel ($d_g \simeq 50$ μm) without helium: (a) 1.55 dpa, (b) 10.85 dpa, (c) type 316 stainless steel, 4.85 dpa.

Table 3

Void Nucleation Data

Specimen	ϕt (dpa)	d_g (μm)	C_v (10^{15} cm^{-3})	d (Å)	Helium Content
RMS-1a	9.30	1.0	0.80	153	0
RMS-1b	1.55	2.60	0.78	123	0
RMS-2a	9.30	0.45	0.24	127	0
type 316	4.65	~ 50	8.37	133	0
RMS-1a	4.65	1.15	1.11	195	10 ppm
RMS-1b	4.65	2.77	3.00	138	"
RMS-1c	4.65	1.73	3.55	164	"
RMS-2a	8.06	0.46	0.52	186	"
RMS-2a	9.92	0.75	1.81	138	"
RMS-2b	8.06	0.80	1.52	186	"

As seen from table 3, voids became distinctly resolvable in large grains at a dose as low as 1.55 dpa (also see fig. 5a) whereas a displacement dose level of up to 9.30 dpa was necessary before voids became clearly observable in small grains; the void size in both cases was of the same order of magnitude although the void number density was much higher in the large grains than in the small ones. A similar effect of grain size was also observed in samples containing helium (table 3 and figs. 6-8).

Another significant aspect of our observations is that the number density of distinctly observable voids increased with increasing displacement dose (see figs. 5 and 7); in some cases the increase continued up to a fairly high dose level (fig. 7). Generally, the larger the grain, the lower was the dose level at which the void number density saturated (compare figs. 5 and 7). It should be emphasized, however, that the grains investigated in the present work cover a rather small range of grain sizes. Nevertheless our experiment shows that in very large grains (~ 50 μm) the void number density saturates very early (at about 4.65 dpa) (see next section) whereas in 0.5 μm grains the void number density does not change with the dose (fig. 6).

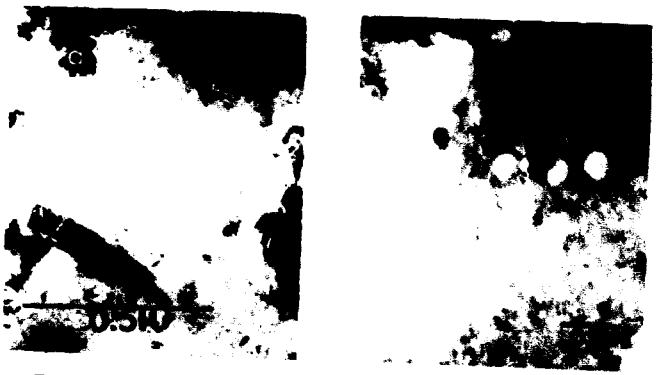

Fig. 6. Voids in RMS-2b stainless steel (d_g = 0.52 μm) with 10 ppm helium: (a) 18.6 dpa (b) 36.41 dpa.

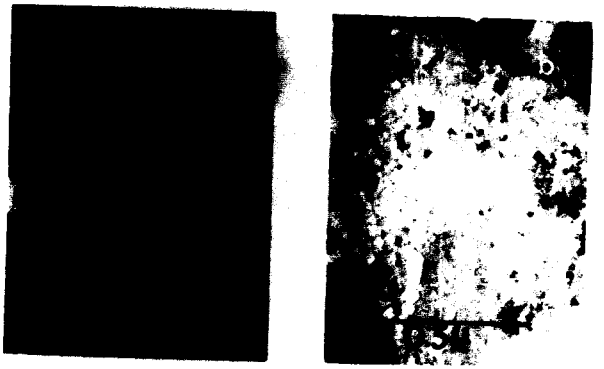

Fig. 7. Voids in RMS-2a stainless steel (d_g = 0.80 μm) with 10 ppm helium: (a) 8.06 dpa, (b) 21.31 dpa.

The role of implanted helium in increasing the void number density is unambiguously clear (compare figs. 5 and 8). It should be noted, however, that the increase was more marked in large than in small grains.

Fig. 8. Voids in RMS-1c stainless steel (d_g = 1.73 μm) with 10 ppm helium at 14.88 dpa.

In samples both with and without helium, the voids were observed to nucleate reasonably uniformly in large (〉1.0 μm) grains (figs. 5 and 8). It should be emphasized, however, that even in the large grains (but without helium), void clustering frequently occurred (figs. 5 (a-b)). In small (〈1.0 μm) grains, on the other hand, the void distribution was almost always non-uniform (figs. 6 and 7). In the samples containing dispersions of aluminium oxide particles, voids always tended to nucleate and grow in cluster form (figs. 6 and 7); the presence of helium seems to have had no influence on the void distribution in these samples. It must be pointed out though that in the dispersed samples the grains were always smaller than about 1.0 μm.

3.2. Swelling and Its Dose Dependence

3.2.1. Void Size

Variations of the average void size with displacement dose for samples with and without helium are shown in figs. 9 and 10, respectively; some selected void size distributions are shown in figs. 11 and 12. In both doped and undoped groups of samples, the effect of grain size on the average void size and on the void growth rate is marked. In undoped and undispersed specimens, for instance, the growth rate during the early stages of irradiation was much faster in the 2.6 μm grain than in the 1.0 μm grain; at higher dose levels the growth rate in both cases reached about the same

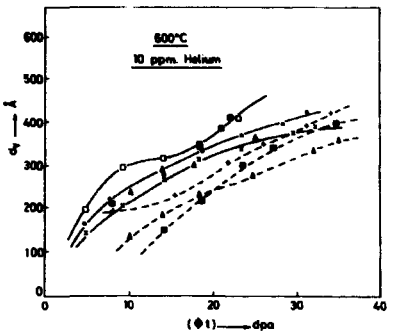

Fig. 9. Variation of average void size, d_v, with dose, φt, in RMS-1 and RMS-2 stainless steels with 10 ppm helium, d_g in μm: x - 2.77 μm (RMS-1b); ● - 1.73 μm (RMS-1c); ▲ - 1.30 μm (RMS-1a); □ - 1.15 μm (RMS-1a); ■ - 0.70 μm (RMS-1a); △ - 0.75 μm (RMS-2a); ▣ - 0.52 μm (RMS-2b); + - 0.46 μm (RMS-2a).

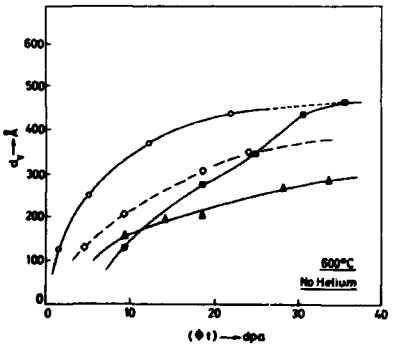

Fig. 10. Same as in fig. 9 but without helium: ◇ - 50 μm (type 316); ○ - 2.60 μm (RMS-1b); ▲ - 1.0 μm (RMS-1a); ■ - 0.45 μm (RMS-2a).

value (fig. 10). As far as the average void size at a given displacement-dose level is concerned, it was found to be much larger in the 2.6 μm grains than in the 1.0 μm grain (fig. 10). The average void size in the 2.6 μm grain was also much larger than in the case of undoped type 316 stainless steel in which grain size was of the order of 50 μm. In the case of undoped and dispersed sample in which a grain of 0.45 μm was irradiated, the initial growth rate was slightly lower than in the 2.6 μm grain but at intermediate doses it became substantially higher, before reaching about the same value as in the 2.6 μm grain at the higher dose levels. In doped but undispersed samples, the initial growth rate was higher in the smaller grain; the average void size at a given dose generally decreased with increasing grain size (fig. 9).

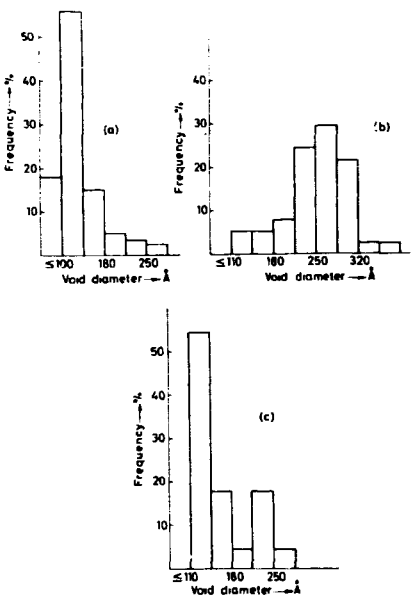

Fig. 11. Void size distribution in samples without helium, d_g in μm: (a) type 316, 4.65 dpa, 50 μm, (b) RMS-1b, 4.96 dpa, 2.60μm, (c) RMS-1a, 9.30 dpa, 1.0 μm.

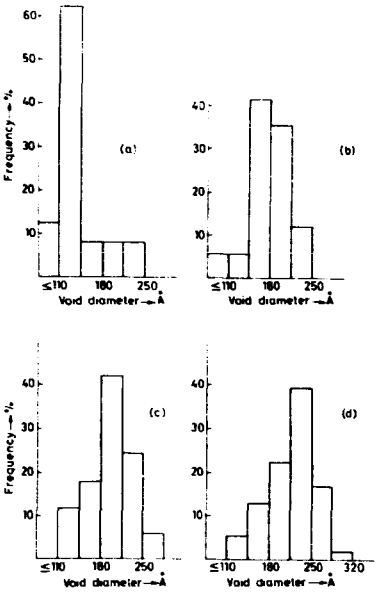

Fig. 12. Same as in fig. 11 but with 10 ppm helium at 4.65 dpa: (a) RMS-1b, 2.77 μm (b) RMS-1c, 1.73 μm (c) RMS-1a, 1.15 μm (d) RMS-1a, 0.70 μm.

In the doped and dispersed specimens, the void growth rate was generally smaller than in the doped and undispersed ones during the early stages of irradiation. It should be noted that up to about 20 dpa there was very little growth of voids in the doped and dispersed samples (fig. 9); the voids in these specimens tended to grow faster at higher doses (⟩ 20 dpa). It is quite clear though that the void size generated in dispersed samples was smaller than in the undispersed ones at all dose levels.

In figs. 13 and 14 the void concentration is plotted against the average void size. The results clearly show that in all the grains larger than ~ 0.5 μm there is a void size at which the void concentration reaches a maximum and then decreases at larger sizes. Generally the peak value of the void concentration decreases and the peak position shifts to higher void sizes with decreasing grain size.

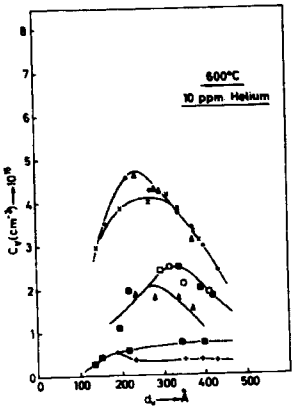

Fig. 13. Variation of void concentration, C_v (cm^{-3}) with average void diameter, d_v; same key as in fig. 9.

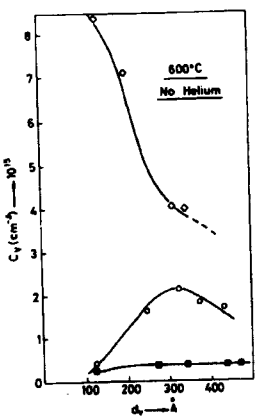

Fig. 14. Same as in fig. 13 but without helium; same key as in fig. 10.

3.2.2. Void Shape

In most of our specimens the voids were observed to have irregular shapes which tend to become nearly spherical at higher doses. However, in one of the large grain specimen containing 10 ppm of implanted helium, voids with regular shape were formed (fig. 8); the grain size in fig. 8 is 1.73 μm. The void shape in type 316 stainless steel, on the other hand, was observed to be regular at all doses (fig. 5c).

3.2.3. Void Concentration

The displacement dose dependence of the void concentration in doped and undoped samples is shown in figs. 15 and 16, respectively. In all specimens the void concentration increased with the displacement dose at least until a dose level of ~10 dpa was reached beyond which it began to decrease. In grains smaller than about 1.0 μm the void concentration continued to increase until displacement dose levels of ≥ 30 dpa were reached.

Up to a dose level of about 10 dpa there was a significant influence of grain size on the void concentration (figs. 15 and 16). Even at higher doses the difference in concentration levels between grains smaller than about 1.0 μm and the bigger ones remained substantial. It is also important to note that the rate of increase in the void concentration with the dose tended to decrease with decreasing grain size in samples both with and without helium; in general, the larger the grains, the smaller is the dose level at which the void concentration maximum is reached.

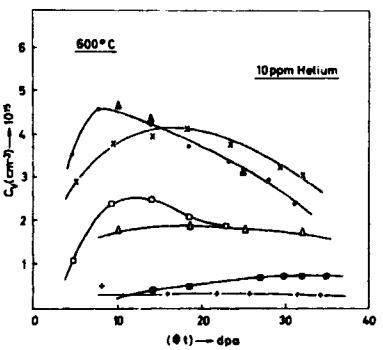

Fig. 15. Variation of void concentration, C_v (cm^{-3}), with dose, Φt, same key as in fig. 9.

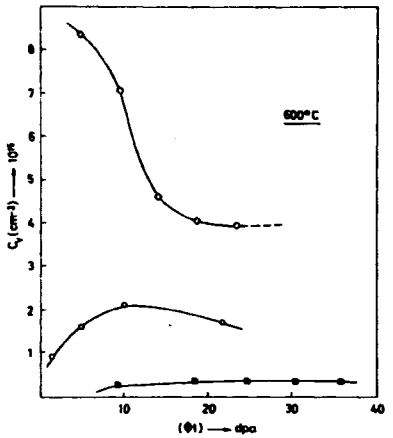

Fig. 16. Same as in fig. 15, but without helium, same key as in fig. 10.

3.2.4. Void Volume

The change in void volume per unit volume of the specimen*, (ΔV/V), is shown in figs. 17 and 18. In almost all samples the larger the grain size, the higher is the void volume at all dose levels. It is also quite clear that, in general, the rate of void volume increase with the dose increased with increasing grain size. Furthermore, for grains smaller than ~ 1.0 μm (i.e. in dispersed specimens), the void volume increase up to ~20 dpa was very small. Beyond this level the rate increased and seems to saturate at about 35 dpa. In the grains of sizes between about 0.70 and 3.0 μm there was a substantial increase in the void volume because of the presence of the implanted helium.

In the specimens containing dispersions of aluminium oxide particles, the presence of helium seems to have had no significant influence on the total void volume in grains of about 0.5 μm size.

*In the computation of (ΔV/V) the presence of void denuded zone is not accounted for - see discussion.

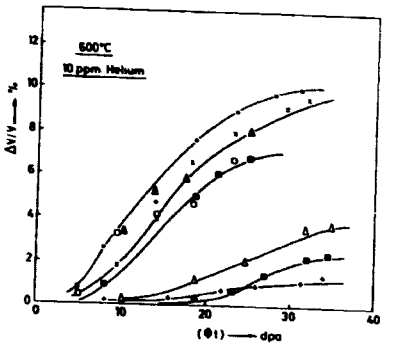

Fig. 17. Dose dependence of swelling (ΔV/V); same key as in fig. 9.

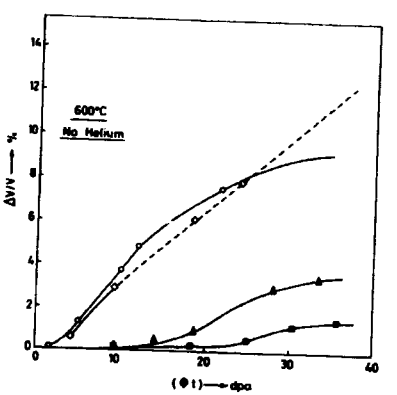

Fig. 18. Same as in fig. 17, but without helium; same key as in fig. 10.

3.2.5. Void Denuded Zone and Grain Boundary Migration

During irradiation the boundaries of the grain being irradiated were frequently found to migrate away from the centre of the grain; the boundary displacement, δ_g, increased with the irradiation dose (fig. 19). The width of the apparent void denuded zone, W'_D, along grain boundaries also increased with the dose, as shown in fig. 19. However, the actual denuded zone width, $W_D = (W'_D - \delta_g)$, was found to remain almost constant during

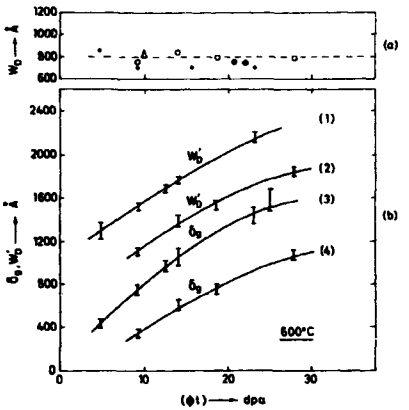

Fig. 19. Variation of grain boundary displacement (δ_g), apparent denuded zone width (W'_D), and actual denuded zone width ($W_D = W'_D - \delta_g$) (d_g in μm) with dose: (a) ∘ - RMS-1a, 1.15 μm, 10 ppm. helium, o - RMS-1a, no helium ●- RMS-1a, 0.7 μm, 10 ppm. helium, Δ - RMS-2a, 0.5 μm, 10 ppm. helium (b) curves (1 and 3), d_g = 1.15 μm (RMS-1a), 10 ppm. helium, curves (2 and 4), d_g = 1.0 μm (RMS-1a), no helium.

irradiation, as it is shown, for grains of different sizes, in fig. 19. Fig. 20 shows the influence of the grain size on the boundary displacement during irradiation of RMS-1a steel with and without implanted helium; the smaller the grains, the smaller was the displacement. The grain growth parameter $(D^2 - D_o^2)$, where D is the grain diameter at any irradiation time t_i and D_o is the initial grain diameter* at $t_i = 0$, is plotted against irradiation time

*D and D_o are measured as the perpendicular distance between two opposite boundaries of a grain.

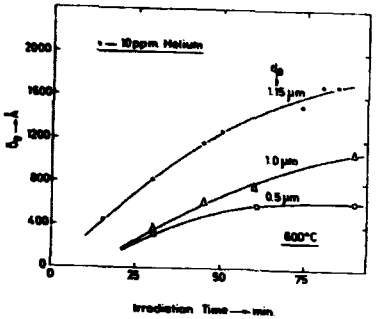

Fig. 20. Effect of grain size on the variation of δ_g with irradiation time in RMS-1a stainless steel.

in fig. 21. The variation of $(\Delta V/V)^*$ for the 1.15 μm grain with the irradiation time is also shown in fig. 21. It is of interest to note two things here: (a) that the boundary displacement rate decreased as the $(\Delta V/V)^*$ rate decreased and (b) that the smaller the $(\Delta V/V)^*$, the smaller was the boundary migration.

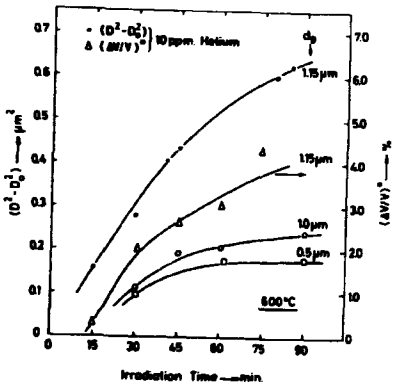

Fig. 21. Variation of $(D^2 - D_o^2)$ and $(\frac{\Delta V}{V})^*$ with irradiation time in RMS-1a stainless steel.

3.2.6. Preferential Void Growth

In some cases the voids situated immediately adjacent to the denuded zone grew faster than those in the grain interior; the void size dependence on the displacement dose of the total void population in the grain interior (without helium) and of six voids adjacent to the denuded zone (in the same grain) is shown in fig. 22. Similar results were also obtained for grains containing helium.

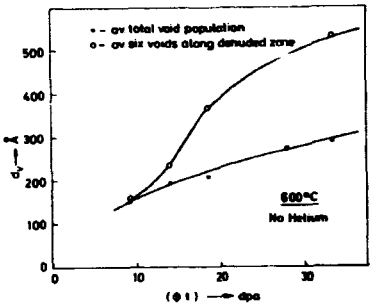

Fig. 22. Void growth with irradiation dose in RMS-1a.

4. DISCUSSION

4.1. General Considerations

Our results described in the previous section clearly suggest that the size of the grain under irradiation plays a significant role in determining the voidage characteristics of the material. Before going into a detailed discussion of this effect and its importance, it is appropriate to consider very briefly the process of defect accumulation which leads to the nucleation of voids.

As mentioned in section 1, the collision between the energetic particles and the target atoms produces vacancies and self-interstitials, provided the energy imparted to the target atoms during the collision event is equal to or greater than the displacement energy. These defects are assumed to be produced at random throughout the lattice. At relatively high temperatures (i.e. $T \geq 0.30\ T_m$) both vacancies and self-interstitials move by random walk through the lattice. During their motion, some of them recombine with their opposite type and cease to exist, and some of them annihiliate

at fixed, biased or neutral sinks; the remainder form clusters which eventually grow into dislocation loops. These dislocation loops as well as the grown-in dislocation lines, attract self-interstitials in preference to the vacancies. The biased attraction of interstitials at dislocations is a direct manifestation of the long range drift interaction between the stress field of dislocations and point defects[17]; the relatively large distortion field associated with an interstitial compared to that with a vacancy ensures that a net interstitial drift will occur and leads to an excess interstitial loss at the dislocations[18]. This causes a rise in the "quasi-steady state" vacancy concentration level and leads to the nucleation of voids and their subsequent growth. The rate as well as the degree of increase in the level of vacancy concentration (i.e. above the thermal equilibrium concentration) in a crystalline solid being irradiated, with a given damage rate, are determined by the number and distribution of biased and neutral sinks present in the solid, neglecting the effects of spatial variations in defect concentration on the mutual recombination of interstitials and vacancies. Clearly, structural parameters such as dislocations, grain boundaries, and precipitates etc. are, therefore, expected to play an important role in determining the damage behaviour of a material. In the following the effect of grain boundaries and the grain size on the nucleation of voids and the concomitant swelling is discussed.

In view of the high defect generation rate and the temperature employed during the present irradiation experiments, the formation of defect agglomerates in the form of black dots and dislocation loops already at $t_i = 0$ is quite understandable. The fact that a sizeable population of black dots and dislocation loops are found to be associated with grown-in dislocation lines at the very early stage of the irradiation clearly demonstrates the efficiency of dislocation lines in trapping interstitial atoms.

Since the voids cannot be distinctly resolved at the time of their nucleation, it is impossible to make a direct assessment of the defect concentration situation which leads to the nucleation of voids. It is thought, however, that some qualitative but valuable knowledge about the nucleation behaviour can be gained from the experimental data on (a) the displacement dose level at which the voids become distinctly resolvable for the first time and the dependence of this level on implanted gas content (b) the size and concentration of the voids when they first appear (c) the dose dependence of the void concentration and (d) the variation of void concentration with the implanted gas content. Some of our results quoted in table 3 clearly suggest that void nucleation is strongly dependant on the size of the grain under irradia-

tion. A similar conclusion can also be reached from the dose dependence of the void concentration in different size grains (figs. 15 and 16). Furthermore, our data (figs. 17 and 18) clearly demonstrate that the void volume swelling consistently decreases with decreasing grain size.

No systematic study of the effect of grain size on void formation has been previously reported in the literature. In the following a model is proposed to explain grain size dependent void formation.

4.2. The Denuded Zone Model

The model is based on the well established fact that grain boundaries act as neutral and unsaturable sinks for vacancies and self-interstitials. The formation of dislocation loop and void denuded zones along grain boundaries is a direct manifestation of defect migration from these zones to the boundaries. The formation of dislocation loop denuded zones has been experimentally observed in quenched[13] as well as in irradiated[14] metals and alloys. There are numerous examples of void denuded zone formation in stainless steel, nickel, and aluminium (ref. 3); an example from our work is shown in fig. 23.

Fig. 23. Void denuded zone along grain boundaries in RMS-1a, at 9.30 dpa.

The denuded zone is assumed to contain a vacancy concentration profiles as shown in fig. 24. Two types of vacancy concentration profiles are considered. First we assume that the profile is such that the vacancy concentration reaches its maximum at $X = W_D$ (fig. 24a) and remains constant in the grain interior. In the second case, the vacancy concentration is assumed to reach its maximum in the grain interior at a distance $X > W_D$ (fig. 24b); in this case the interaction between vacancy concentration profiles from opposite grain boundaries of the grain is also considered.

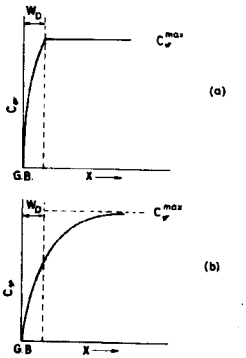

Fig. 24. Schematic representation of the variation of vacancy concentration in a grain (within and beyond the denuded zone) with the distance x from the grain boundary: (a) when $C_v^{max.}$ is reached at $X = W_D$ and (b) when $C_v^{max.}$ is reached at $X > W_D$.

We consider a spherical grain of diameter d_g with a void denuded zone of width W_D at a given irradiation temperature (fig. 25). Assuming that W_D is not a function of d_g, it can be shown that

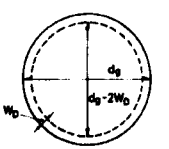

$$\left(\frac{\Delta V}{V}\right)^{*} = \left(\frac{\Delta V}{V}\right)\left[\frac{(d_g - 2W_D)}{d_g}\right]^3$$

Fig. 25. A spherical grain of diameter d_g with a denuded zone of width W_D.

$$\left(\frac{\Delta V}{V}\right)^{*} = \left(\frac{\Delta V}{V}\right)\left\{\frac{(d_g - 2W_D)}{d_g}\right\}^3 \qquad (1)$$

where $\left(\frac{\Delta V}{V}\right)^{*}$ is the swelling representative of the whole grain and $\left(\frac{\Delta V}{V}\right)$ is the actual swelling that occurs in the grain interior of diameter $(d_g - 2W_D)$. Assuming that the voidage characteristics of the grain interior are not altered in any significant way by changing the grain size, it can be seen from eqn. (1) that the overall swelling in the bulk material will be a function of the grain size of the material; the dependence of $\{(d_g - 2W_D)/d_g\}^3$ on d_g is shown in fig. 26. The theoretical curve in fig. 26 is computed on the basis of the experimentally observed value of 0.08 μm for W_D (fig. 19a). Fig. 26 suggests that in grains larger than about 5.0 μm the effect of grain size on the overall swelling $(\Delta V/V)^{*}$ would not be very significant. However, the grain size effect becomes increasingly more important as the grain size decreases below about 5.0 μm.

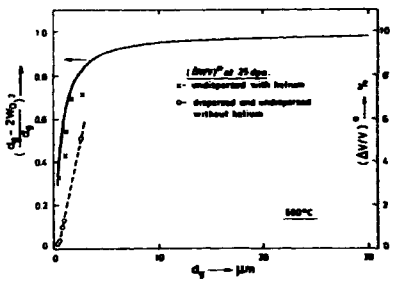

Fig. 26. Grain size dependence of $\{(d_g - 2W_D)/d_g\}^3$ and $(\Delta V/V)^{*}$.

It must be emphasized, however, that the assumption that the voidage characteristics of the grain interior remain unaltered as the grain size changes does not hold for grains below about 5.0 μm. A clear demonstration of this is provided by our experimental results (figs. 15 and 16) which show that the void number density in the grain interior decreases very markedly with decreasing grain size. This would immediately suggest that $\left(\frac{\Delta V}{V}\right)^{*}$ for grains smaller than about 5.0 μm would be less than that predicted by eqn. (1). From our measured values of $\left(\frac{\Delta V}{V}\right)$ and W_D, $\left(\frac{\Delta V}{V}\right)^{*}$ have been obtained using eqn. (1) and their variation with d_g is also shown in fig. 26;

the dose dependence of $\left(\frac{\Delta V}{V}\right)^{*}$ is shown in figs. 27 and 28. The $\left(\frac{\Delta V}{V}\right)^{*}$ values obtained from our experiments and plotted in fig. 26 clearly show that these values are indeed smaller than expected from eqn. (1) for grains

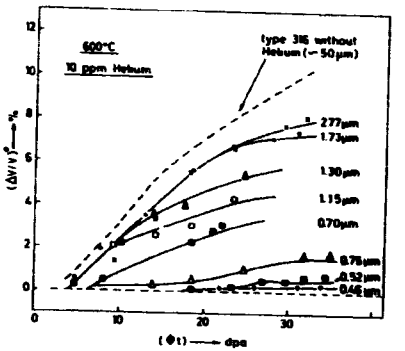

Fig. 27. Variation of $(\Delta V/V)^{*}$ with dose for various grain sizes: x - 2.77 μm (RMS-1b); ● - 1.73 μm (RMS-1c); ▲ - 1.30 μm (RMS-1a); □ - 1.15 μm (RMS-1a); ■ - 0.70 μm (RMS-1a); △ - 0.75 μm (RMS-2a); ▣ - 0.52 μm (RMS-2b); + - 0.46 μm (RMS-2a).

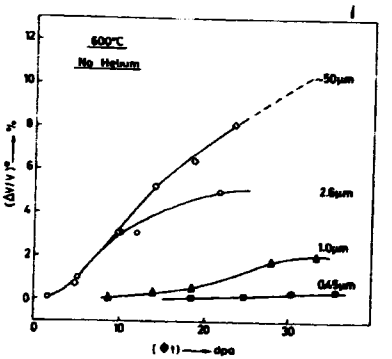

Fig. 28. Same as in fig. 27 but without helium; ◇ - 50 μm (type 316); ○ - 2.60 μm (RMS-1b); ▲ - 1.0 μm (RMS-1a); ■ - 0.45 μm (RMS-2a).

smaller than about 5.0 μm. It is also important to note that the increase in $(\frac{\Delta V}{V})^*$ with grain size (fig. 26) is faster in the specimen containing 10 ppm. of helium than for specimens without helium.

The fact that the void number density in the grain interior decreases with the grain size would indicate that the level of maximum vacancy supersaturation achieved (at a given dose) decreases with the grain size. Another possible explanation could be that the concentration of the impurity gas atoms decreases with decreasing grain size because they can diffuse out to the grain boundaries, and hence the smaller the grains, the lower the void number density. However, results of helium-release measurements (after 300 KeV implantation) in types 304L, 309, and 316 stainless steels[19], show that the mobility of helium is very low up to about 800°C in types 304 and 309 and up to 700°C in type 316 stainless steel in the concentration range of 10^{-5} to 10^{-2} atom fraction. Our specimens contain only 10^{-5} atom fraction (i. e. ≃ 10 ppm.) of helium and have been heated to 600°C before irradiation commenced. It seems highly unlikely therefore that any substantial release of helium will occur in our specimens during the heating-up period. It is possible that helium atoms might become mobile during irradiation. However, it is important to note that the vacancies are highly mobile during irradiation at 600°C and therefore it is difficult to comprehend the reason why helium atoms would migrate to the grain boundaries, in preference to the vacancies, from the whole grain (i. e. the denuded zone as well as the grain interior).

Besides, the probability of helium atoms diffusing out to grain boundaries in a grain of ~ 0.5 μm dia. is the same as to surfaces in a thin foil of about 0.5 μm thickness. The high voltage electron irradiation experiments on thin foils (~ 0.5 μm thick) of metals and alloys have demonstrated, however, that the void number density increases with increasing amount of helium atoms implanted prior to irradiation; our results for larger grains celarly show the effect of implanted helium (compare figs. 5 and 8). The suggestion that helium atoms might migrate to the grain boundaries (from the grain interior), therefore, does not seem credible.

It would thus appear that the decrease in the void number density in smaller grains is caused by the lower vacancy supersaturation. A lower vacancy supersaturation in the grain interior of smaller grains could be caused by the existence of vacancy concentration gradients from the grain boundaries into the grain interior, as shown schematically in figs. 24b and 29. In neutron irradiated nickel 270 it has been observed by Stiegler and Bloom[16] that the void number density gradually increased to its maximum

at a distance of about 1.0 μm from the grain boundary and did not suddenly rise to its maximum immediately beyond the denuded zone (W_D = 0.1 μm); this would also suggest the existence of a concentration gradient extending beyond X = W_D (i. e. as in figs. 24b rather than 24a).

The existence of such profiles extending beyond X = W_D (fig. 24b), their possible interactions and the consequences thereof are schematically illustrated in fig. 29. Three points should be noted here: (a) that the vacancy concentration goes up as the irradiation continues, (b) that the interaction between the vacancy concentration gradients from the two boundaries leads to a decrease in the level of vancancy concentration in the grain interior, and (c) that the smaller the grain, the lower is the vacancy concentration level in the grain interior at a given irradiation time (i. e. dose). In the above consideration, the recombination rate of vacancies and self-interstitials is assumed to remain the same for different grain sizes.

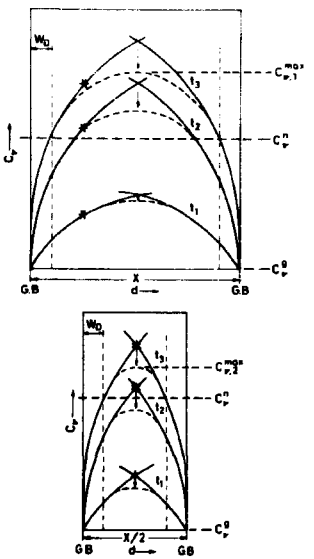

Fig. 29. Increasing vacancy concentration, C_v, with irradiation time, t_i, and its variation with distance, d, from the grain boundary: (a) when d_g = x and (b) when d_g = x/2; C_v^e = equilibrium vacancy concentration in the grain boundary, C_v^n = vacancy concentration necessary for the nucleation of voids to occur, $C_v^{max.}$ = maximum vacancy concentration achieved.

The present model, therefore, predicts that the void volume swelling will decrease with decreasing grain size (eqn. 1) and that a further reduction in swelling can be expected in very small grains where concentration profile interaction is possible. The tentative conclusion of the model that the smaller the grain, the lower the vacancy concentration prevailing at a given time of irradiation, would predict that the nucleation of voids will also be affected by the grain size.

It must be emphasized, however, that the model remains only qualitative and therefore its predictions cannot be assessed quantitatively. Furthermore, it is not possible at the moment to include the effect of the presence of vacancy concentration gradients beyond $X = W_D$ directly and quantitatively on the dependence of $(\frac{\Delta V}{V})^*$ on d_g.

It is also worth pointing out the possibility that a higher dislocation density (grown-in and irradiation-induced) in smaller grains can also cause a decrease in the void number density in the grain interior; the effect would be similar to that caused by cold deformation[20]. However, our experiments so far have not provided any conclusive evidence for or against the grain size dependence of dislocation density during irradiation. Besides, the critical dislocation density above which the increase in dislocation density can become deleterious for voidage (i. e. can increase vacancy concentration instead of decreasing it) will have to be calculated and experimentally determined before any quantitative assessment of this effect on the vacancy concentration and the void number density in the grain interior can be attempted.

4.3. Void Nucleation

Assuming that $\dot{n}_v^c > (\dot{n}_v^a + \dot{n}_v^r)$ where $\dot{n}_v^c$ is the rate of creation, n_v^a the rate of annihilation, and $\dot{n}_v^r$ the rate of mutual recombination of vacancies, the vacancy concentration in the grain under irradiation is expected to increase with increasing dose (for a given damage rate). It follows from the previous section that in the size range where d_g is comparable to $2W_D$, the smaller the grain, the higher would be the dose necessary to reach the vacancy concentration level, C_v^n, required for the nucleation of voids (see fig. 29), and the lower would be the level of maximum vacancy concentration, $C_v^{max.}$, reached in the grain interior.

Our results show that generally the smaller the grain, the higher is the dose level required for the voids to become observable for the first time (table 3). Furthermore, it is found that the smaller the grain, the lower is the void number density both at the time when they are first observed (table 3) and at higher doses (figs. 15 and 16); the implantation of helium atoms does not change this behaviour. These results are consistent with the predictions of the model outlined above and in the previous section.

In the specimens which contain the necessary amount of helium for void-nuclei-stabilization, it is reasonable to expect that the nucleation of voids should occur at rather an early stage. This is actually observed experimentally but only in relatively large grains (table 3). The nucleation event in the smaller grains, on the other hand, is invariably delayed. This would tend to suggest that the stabilization of vacancy clusters into viable void nuclei is dependent on the level of vacancy supersaturation, such that those clusters which have grown beyond the critical size range can be stabilized into viable void nuclei. Alternatively, a lower void number density in smaller grains could arise if lower vancancy supersaturation requires a higher number of impurity-gas atoms in order to stabilize vacancy clusters of a given size. The experimental observations (a) that the nucleation of voids in smaller grains with as well as without implanted helium continues until a relatively high dose level is reached, and (b) that the dose level at which the nucleation saturated is higher for smaller grains (figs. 15 and 16) can also be explained by the suggestions outlined above. The fact that the addition of helium increases the void number density in relatively larger grains and has virtually no influence in very small grains is also consistent with the present argument in that the vacancy supersaturation level is expected to be lower in the smaller grains (section 4. 2).

It is not possible at the moment to ascertain directly whether the delayed nucleation is a result of inefficient stabilization of vacancy clusters or of a slow growth rate of stabilized clusters in their critical size range. Nonetheless, it is worth noting that void growth follows a parabolic relationship with irradiation dose (i. e. time), in all grains, and that the extrapolation of the growth line for different size grains to $d_v = 0$ (d_v is the average void diameter) clearly suggests that the smaller the grain, the larger is the dose at which $d_v = 0$[21]. Thus it seems that the delayed nucleation results from inefficient stabilization and not from a slow growth rate of the void embryos (i. e. stabilized vacancy clusters).

The role of the dispersed non-coherent particles in the void nucleation process is not quite clear primarily because none of the grains irradiated contained particles in the grain interiors; the particles are almost always situated at the grain boundaries.

4.4. Void Swelling and Its Dose Dependence

One of the consequences of the formation of voids in a crystalline solid is that the solid expands in volume by an amount exactly equivalent to the volume of the voids in it. The dose dependence of this swelling at a given temperature is determined, of course, by the dose dependence of both the void number density and the void size. In the following we, therefore, first consider the dose dependence of the void size and the void concentration individually and thereafter the dose dependence of the swelling itself.

4.4.1. Void Growth

A net flux of vancancies (i. e. greater than that of self-interstitials) must reach the growing voids. At a given temperature and under a given set of irradiation conditions, the net flux of vacancies that can be available to each void depends on several factors (dislocation density, void density etc.). For example, the net flux is expected to get smaller as the number density of voids increases. Hence, the higher the void concentration, the lower the growth rate. This implies that at a given dose level, the lower the void concentration, the larger will be the void size.

Our void growth results fall into two groups according to the size of the grain under irradiation. For grains larger than about one micron, the results are consistent with the above mentioned argument in that the growth rate increases as the void concentration decreases in grains of sizes between 1.15 - 2.77 μm (fig. 9). The comparison with the results for type 316 stainless steel, however, shows that although there is a noticeable difference in the void concentration between type 316 (undoped) and the 2.77 μm grain containing helium (fig. 16) yet the growth rate in both cases is very much the same (fig. 10). Another point to note is that the growth rate in an undoped 2.60 μm grain is much higher than in an undoped 1.0 μm grain although the maximum void concentration in both cases is of the same order of magnitude. This would suggest that the reduction in grain size (particularly in the size range used in the present investigation) lowers the vacancy supersaturation in the grain interior and hence the flux to the growing voids.

In the second group are our results on doped grains in the size range between about 0.5 μm to 1.0 μm (fig. 9). It is interesting to note that in grains within this size range, the growth rate decreases, as in the previous case, as the void concentration increases. However, the growth rate in the 0.75 μm grain is about the same as in the 2.77 μm grain (both grains are doped) whereas the difference in the void concentration between the two grains is enormous (see fig. 15). This, once again, indicates that the decrease in grain size is responsible for the reduced level of vacancy supersaturation in the grain interior leading to slower growth rate. The evidence that the smaller the grain, the lower the $C_v^{max.}$ and larger the d_v at which $C_v^{max.}$ is reached (figs. 13 and 14) also support the above assertion.

4.4.2. Void Concentration

The most pronounced effect of the grain size in our experiments is on the void concentration (figs. 15 and 16). It should be noticed that even in the doped 2.77 μm grain the void number density is substantially lower than in the case of similarly irradiated type 316 stainless steel with about 50 μm grain size; this has already been considered in the previous section.

The void concentration in undoped type 316 is found to saturate at a rather low dose level whereas in our fine-grained specimens, doped or undoped, the saturation occurs invariably at much higher doses (figs. 15 and 16). It is anticipated that in general void nucleation will essentially cease when the void concentration reaches a level at which the voids' spheres of influence (i. e. the volume containing the vacancy gradient to the void surface) begin to impinge upon each other i. e. at a level for which the probability that vacancies will jump into a void exceeds the probability that they will form a new void nucleus. Since the void's sphere of influence increases with increasing mobility (i. e. irradiation temperature), nucleation is expected to saturate at a lower dose (i. e. maller void concentration) at relatively high irradiation temperatures. Our results on undoped type 316 stainless steel (fig. 16) show, for example, that void nucleation at 600°C does indeed saturate at a low dose level. The prolonged nucleation up to high doses observed in our small grains (see previous section) would indicate that the number of void embryos which can be stabilized into three-dimensional configurations must increase with dose.

It is not quite clear at this stage whether all impurity gas atoms are first consumed in stabilizing some void embryos at the low vacancy concentration level (i. e. low dose) and then as the dose increases some of them are knocked out of the stabilized void nuclei and help stabilize the new embryos in the subcritical size range or whether the impurity atoms become associated with a lot more vacancy clusters and only a few of them ever grow beyond the critical size range to become real voids.

4.4.3. Void Swelling

An unambiguous demonstration of the grain size effect on the dose dependence of the void volume is shown in figs. 27 and 28. It is interesting to note here that in grains with $d_g > 1.0$ μm the rate of increase in the void volume with dose is roughly the same up to about 10 dpa. Beyond this dose level, the void-volume-increase with dose begins to slow down with decreasing grain size; the larger the grain size, the higher is the dose up to which the high rate of volume increase prevails. It should also be emphasized that even in the 2.77 μm grain containing 10 ppm. of helium the void volume increase saturates at much lower dose level than in the undoped 316 stainless steel.

In view of what has been said in section 4.2 (see also fig. 26), the grain size effect on the void volume is not altogether surprising. What is not clearly understood is the fact that in samples containing dispersions of aluminium oxide particles the void swelling for a given grain size (admittedly limited only to a small size range, i.e. 0.5 to 0.8 μm) and at a given dose level is always noticeably smaller than in samples without dispersions. As mentioned before the dispersed particles are always present at the grain boundaries and not in the grains. The incoherent interfaces between the aluminium oxide particles and the stainless steel matrix are expected to act as non-preferential and effective sinks for both vacancies and self-interstitials. However, when these particles are situated at the grain boundaries which act as sinks themselves it is very difficult to analyse the role of these interfaces in reducing the voidage level in the grain interiors.

4.4.4. Denuded Zone and Grain Boundary Migration

The actual void denuded zone width, W_D is found to remain almost constant at doses used in the present investigation (fig. 19a), whereas the grain boundary displacement, δ_g, increases with the dose (fig. 19b). It seems quite obvious from fig. 19, therefore, that the increase in the apparent denuded zone width, W'_D, with the irradiation dose is caused exclusively by grain boundary migration; fig. 19a also tends to suggest that the size of the denuded zone width, W_D is independent of the grain size.

In view of the suggestion made by several authors[22-27] that the mobility of grain boundaries is strongly influenced by vacancies, our observation of grain boundary migration is not very surprising since the irradiation-induced defects are readily available to the boundaries. The unusual aspect of our results is the directionality of the boundary migration. Fig. 23, as

well as many other such examples, clearly demonstrates that in our case the boundary migration occurs from the irradiated side to the unirradiated side.

This seems to be caused by the fact that during irradiation the mobile boundaries receive not only vacancies but also self-interstitial atoms; in fact, more self-interstitial atoms than vacancies are likely to migrate to the boundaries which results in a net flux of self-interstitial atoms arriving at the grain boundaries. Exactly how the arrival of these self-interstitial atoms at the grain boundaries affects their migration is not quite clear. However, the observed directionality of the boundary migration can be reasonably well understood if it is accepted that the self-interstitial atoms, upon their arrival at the grain boundary, join the parent lattice instead of becoming "boundary atoms" and diffusing along or across the boundary.

On the basis of the idea outlined above, the boundary displacement in our case would be expected to depend on the arrival of the flux of self-interstitial atoms to the boundary. Our results (figs. 20 and 21) show that the boundary displacement rate slows down as irradiation progresses. The void swelling rate also decreases with increasing irradiation time (figs. 21, 26, and 27), and reflects the fact that the net flux of vacancy supply to the growing voids decreases with the dose. This, in turn, means that the net flux of self-interstitial atoms arriving at the migrating boundaries decreases as irradiation continues; hence the decreased boundary migration rate.

The fact that boundary migration is strongly influenced by the size of the grain being irradiated (fig. 20) can also be readily explained in terms of the above mentioned idea. Observations clearly show (fig. 27) that void volume swelling is substantially reduced by reducing the size of the grain, This would imply that the net flux of interstitial atoms to the boundary decreases with decreasing grain size and hence the smaller the grain, the lower should be the migration rate, and this is what we observe experimentally (fig. 20).

In considering boundary displacement particularly in relatively large grains in which a substantial amount of void volume swelling occurs, the role of the hydrostatic stress, induced by this swelling and acting on the boundaries in the direction away from the centre of the grain, must also be taken into account. It seems most likely, however, that the presence of this hydrostatic stress is not a dominant factor in controlling boundary displacement because boundary displacement is observed even in the absence of this stress (i.e. when $(\Delta V/V) = 0$, 0.5 μm grain, fig. 20).

5. CONCLUSIONS

1. The investigation clearly demonstrates that our "experimental" stainless steel is a highly void swelling resistant material which may be considered as an attractive candidate material for the fast breeder reactor application.

2. The swelling resistance is found to be due mainly to the grain refinement and the presence of dispersed particles.

3. Both in undoped and helium doped samples of dispersed and undispersed stainless steel void formation is completely suppressed in grains smaller than about 0.4 μm.

4. A "Denuded Zone Model" is proposed to explain grain size dependent void volume swelling.

5. The model also explains the nucleation behaviour observed in the present investigation. It seems very likely that the stabilization of three-dimensional vacancy clusters into viable void nuclei is determined not only by the presence of impurity atoms but also by the level of vacancy supersaturation (i.e. the size of vacancy clusters) in the grain under irradiation.

6. The void nucleation event is found to be considerably delayed in grains with $d_g \lesssim 1.0$ μm, where d_g is the grain diameter.

7. The void number density (at a given dose level) tends to decrease with grain size.

8. The dose dependence of void number density demonstrates that void nucleation in smaller grains continues up to much higher doses; in larger grains the nucleation of voids ceases to occur at much lower doses.

9. Void growth is found to be influenced by the concentration of voids.

10) Void nucleation behaviour of small grains ($d_g < 1.0$ μm) remains unchanged even when helium is implanted in them prior to irradiation.

11) The swelling and its dose dependence are found to be strongly dependent on the size of the grain under irradiation; in the size range 0.45 to ~ 3.0 μm the smaller the grain, the lower is the swelling.

12) The effect of grain size and particles on void volume swelling is retained also in the presence of implanted helium. For a given grain size void volume swelling is found to be smaller in the dispersed than in the undispersed stainless steel even though the dispersed particles are always intergranular.

13. Irradiation-induced dislocation loops associated with grown-in dislocations or grain boundaries are found to grow exclusively in their length direction; the vast majority of these loops are aligned in their length direction.

14. During irradiation, grain boundaries are found to migrate away from the centre of the grain; this seems to be caused by the arrival of a net flux of self-interstitial atoms at the grain boundaries.

ACKNOWLEDGEMENTS

The author is grateful to Prof. L. T. Chadderton and Dr. J. B. Bilde-Sørensen for their valuable help in carrying out some of the experiments mentioned in this report. I am also grateful to Dr. N. Hansen for his continued interest in the programme.

I would like to thank Drs. M. J. Makin, A. J. E. Foreman, J. H. Evans, M. R. Warren, and Mr. T. Leffers for several constructive discussions and Messers J. Lindbo and P. Nielsen for their help in producing the specimens.

REFERENCES

1) Cawthorne, C., and Fulton, E. J., Nature 216 (1967) 575.

2) Pugh, S. F., Loretto, M. H. and Norris, D. I. R., Eds. "Voids Formed by Irradiation of Reactor Materials", Proc. B. N. E. S. European Conf., Reading, 24-25 March, 1971.

3) Corbett, J. W. and Ianniello, L. C., Eds. "Radiation Induced Voids in Metals", Proc. Int. Conf., Albany, State University of New York, 9-11 June, 1971.

4) Norris, D. I. R., Radiat. Eff. 14 (1972) 1; 15 (1972) 1.

5) Bullough, R. and Lidiard, A. B., Comm. Solid State Phys. 4 (1972) 69.

6) Seeger, A., Comm. Solid State Phys. 4 (1972) 79.

7) Katz, J. L., and Wiedersieh, H., J. Chem. Phys. 55 (1971) 1414; also in ref. 3, p. 825.

8) Russell, K. C., Acta Met., 19 (1971) 753.

9) Russell, K. C., and Powell, R. W., Radiat. Eff. 12 (1972) 127.

10) Burton, J. J., Scripta Met. 5 (1971) 449.

11) Bullough, R., and Perrin, R. C., in "Radiation Damage in Reactor Materials", vol. II, IAEA, Vienna, 1969, p. 233.

12) Harkness, S. D., and Li, Che-Yu, Met. Trans. 2 (1971) 1457.

13) Hirsch, P. B., Silcox, J., Smallman, R. E., and Westmacott, K. H., Phil. Mag. 3 (1958) 897.

14) Stiegler, J. O. and Bloom, E. E., Radiat. Eff. 8 (1971) 33.

15) Singh, B. N., J. Nucl. Mat., 46 (1973) 99.

16) Lindbo, J. and Leffers, T., Metallography 5 (1972) 413.

17) Bullough, R., and Newman, R. C., Rept. Prog. Phys., 33 (1970) 101.

18) Bullough, R., AERE (Harwell) Rept. TP-375, 1969.

19) Bauer, W., and Wilson, W. D., ref. 3, p. 230.

20) Walters, G. P., in ref. 2, p. 223 and 231.

21) Singh, B. N., to be published.

22) Coble, R. L., and Burke, J. E., Progress in Ceramic Science, Pergamon Press, 3 (1963) 197.

23) Alexander, B., and Balluffi, R. W., Acta Met. 5 (1957) 666.

24) Dahl, W., and Geissler, J., Zeitschrift f. Metallk. 51 (1960) 42.

25) Gleiter, H., Acta Met. 17 (1969) 565; also p. 853.

26) Cottrell, A. H., in "Dislocations and Plastic Flow in Crystals", Clarendon Press, Oxford, 1953, p. 188.

27) Gleiter, H., and Chalmers, B., in "High-Angle Grain Boundaries", Progress in Materials Science, Pergamon Press, Oxford, vol. 16, 1972, p. 127.

ISBN 87 550 0192 0